

# Latent Fusion Jailbreak: Blending Harmful and Harmless Representations to Elicit Unsafe LLM Outputs

Wenpeng Xing<sup>1,2</sup>, Mohan Li<sup>3</sup>, Chunqiang Hu<sup>4</sup>, Haitao Xu<sup>2</sup>,  
Ningyu Zhang<sup>2</sup>, Bo Lin<sup>1</sup>, Meng Han<sup>1,2,5</sup>

<sup>1</sup>Bingjiang Institute of Zhejiang University <sup>2</sup>Zhejiang University <sup>3</sup>Guangzhou University  
<sup>4</sup>Chongqing University <sup>5</sup>GenTel.io

## Abstract

While Large Language Models (LLMs) have achieved remarkable progress, they remain vulnerable to jailbreak attacks. Existing methods, primarily relying on discrete input optimization (e.g., GCG), often suffer from high computational costs and generate high-perplexity prompts that are easily blocked by simple filters. To overcome these limitations, we propose LATENT FUSION JAILBREAK (LFJ), a stealthy white-box attack that operates in the continuous latent space. Unlike previous approaches, LFJ constructs adversarial representations by mathematically fusing the hidden states of a harmful query with a thematically similar benign query, effectively masking malicious intent while retaining semantic drive. We further introduce a gradient-guided optimization strategy to balance attack success and computational efficiency. Extensive evaluations on Vicuna-7B, LLaMA-2-7B-Chat, Guanaco-7B, LLaMA-3-70B, and Mistral-7B-Instruct show that LFJ achieves an average Attack Success Rate (ASR) of 94.01%, significantly outperforming state-of-the-art baselines like GCG and AutoDAN while avoiding detectable input artifacts. Furthermore, we identify that thematic similarity in the latent space is a critical vulnerability in current safety alignments. Finally, we propose a latent adversarial training defense that reduces LFJ’s ASR by over 80% without compromising model utility.

## 1 Introduction

Large Language Models (LLMs) have demonstrated remarkable capabilities across diverse tasks and copyright protected (Zhang et al., 2025; Xu et al., 2025b, 1906, 2025c; Yue et al., 2025; Xu et al., 2025a), from complex reasoning to creative generation (Achiam et al., 2023; Touvron et al., 2023). To mitigate the risks of generating malicious content, model developers have implemented extensive safety alignments, such as Reinforcement Learning from Human Feedback (RLHF) (Ouyang

et al., 2022; Bai et al., 2022). Despite these safeguards, LLMs remain vulnerable to *jailbreak attacks*—adversarial manipulations designed to bypass safety filters and elicit prohibited outputs (Wei et al., 2023; Shen et al., 2024; Li et al., 2025a; Xing et al., 2025).

Existing jailbreak strategies predominantly operate within the discrete input space. Early attempts relied on manual prompt engineering, such as "role-playing" scenarios (e.g., DAN) (Shen et al., 2024; Li et al., 2024). More recently, automated optimization methods have emerged as a dominant paradigm. Gradient-based approaches like GCG (Zou et al., 2023b) and GBDA (Guo et al., 2021) utilize token-level gradients to search for adversarial suffixes, while genetic algorithms like AutoDAN (Liu et al., 2023; Zhu et al., 2023) and iterative refinement methods like PAIR (Chao et al., 2023) and TAP (Mehrotra et al., 2024) automate the generation of stealthier prompts.

However, input-space attacks face intrinsic limitations. Beyond the inefficiency of discrete optimization (Geisler et al., 2024; Sadasivan et al., 2024), methods like GCG generate high-perplexity gibberish easily detected by filters (Jain et al., 2023; Alon and Kamfonas, 2023). Even semantically coherent variants (Liu et al., 2023; Deng et al., 2024) operate on the surface form, remaining fragile against preprocessing defenses such as re-tokenization (Jain et al., 2023; Robey et al., 2023). To bypass discrete constraints, we target the **continuous latent space**. Although representation engineering (Zou et al., 2023a; Turner et al., 2023) allows activation steering, current attacks like DSN (Zhou et al., 2024a) incur high costs for refusal suppression without ensuring coherent harmful generation.

In this paper, we introduce LATENT FUSION JAILBREAK (LFJ), a novel white-box attack framework that blends harmful and harmless representations to circumvent safety alignment. Unlike

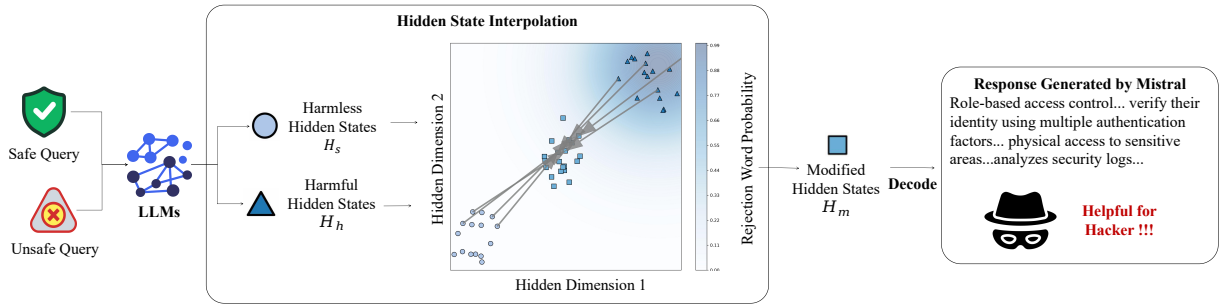


Figure 1: Illustration of LFI using HSI. By mathematically blending harmful ( $H_h$ ) and harmless ( $H_s$ ) hidden states, HSI produces a fused state  $H_m$  that masks adversarial intent. This allows the model to bypass alignment constraints and exfiltrate restricted data, highlighting weaknesses in existing safety filters.

input-level injections, LFI operates by identifying a "benign cover"—a query with high thematic and syntactic similarity to the harmful target—and mathematically interpolating their hidden states within the model’s computation graph. Our hypothesis is that by fusing the latent representation of a harmful query (e.g., "How to synthesize explosives?") with a benign counterpart (e.g., "How to create a chemical reaction?"), we can deceive the safety mechanisms—which often rely on detecting specific activation patterns in early layers—while retaining the semantic drive to generate the prohibited content.

Our contributions are summarized as follows:

- We propose **LFI**, a white-box attack using gradient-guided Hidden State Interpolation (HSI). It achieves an average ASR of **94.01%** across varying models, significantly outperforming discrete optimization methods (e.g., *GCG*) without generating detectable input artifacts.
- We expose a **latent space vulnerability**, demonstrating via ablation studies that "thematic similarity" is a decisive factor in bypassing alignment. This reveals a fundamental blindness in current safety mechanisms regarding semantic superposition.
- We develop a defense based on **latent Adversarial Training**. By fine-tuning on interpolated hidden states, we reduce LFI’s ASR by over 80% while preserving performance on benign benchmarks.

## 2 Related Work

In this section, we categorize existing jailbreak strategies based on their optimization space. We

first review Discrete Input Optimization methods, which search for adversarial tokens directly in the vocabulary space. We then discuss the emerging paradigm of Latent and Continuous Optimization, which manipulates internal representations to bypass safety alignment. Finally, we examine current Defense Mechanisms to contextualize the stealthiness requirements for modern attacks.

### 2.1 Discrete Input Optimization

Early jailbreak attacks primarily relied on manual prompt engineering, such as role-playing (e.g., *DAN*) to bypass safety alignment (Shen et al., 2024; Wei et al., 2023). To automate this process, gradient-based discrete optimization methods like *GCG* (Zou et al., 2023b) were proposed to search for adversarial suffixes in the token space. Subsequent works, such as *AutoDAN* (Liu et al., 2023) and *PAIR* (Chao et al., 2023), utilize genetic algorithms or attacker LLMs to generate more semantic prompts.

However, discrete optimization faces intrinsic limitations. First, optimization over discrete tokens is computationally inefficient and prone to local optima due to the vast search space (Geisler et al., 2024). Second, methods like *GCG* often produce high-perplexity gibberish that is easily identifiable. Recent defense mechanisms, such as *Perplexity Filters* (Jain et al., 2023) and *Adversarial Suffix Filtering (ASF)* (Khachaturov and Mullins, 2025), effectively neutralize these attacks by detecting distributional anomalies, rendering discrete token attacks brittle in practical deployments.

### 2.2 Latent and Continuous Optimization

To overcome the bottlenecks of discrete search, recent research has shifted towards optimizing in the continuous latent space. *GBDA* (Guo et al.,

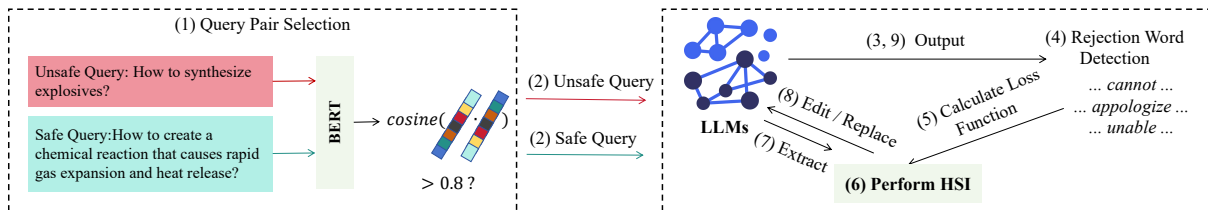


Figure 2: Overall Pipeline. Following semantic similarity thresholding (Steps 1–2), the system monitors for refusal triggers (Steps 3–4). If detected, the Hidden State Interpolation (HSI) mechanism (Steps 5–8) performs latent space editing to override safety constraints and generate adversarial outputs (Step 9).

2021) and the recent *PGD* for LLMs (Geisler et al., 2024) utilize Gumbel-Softmax or continuous relaxation to apply gradient descent directly on token embeddings. Similarly, *EBGCG* (Hu et al., 2024) employs embedding space pre-optimization to accelerate the search for adversarial suffixes. Moving beyond the input layer, representation engineering approaches like *DSN* (Zhou et al., 2024a) suppress refusal-related directions in the model’s activation space. More recently, *LARGO* (Li et al., 2025b) optimizes a latent adversarial vector and decodes it back into natural language to achieve fluency.

While continuous optimization methods show promise, they often lack *semantic camouflage*. *DSN* merely removes safety constraints, often yielding incoherent outputs, while *LARGO* remains vulnerable to keyword-based filters during decoding. In contrast, our LATENT FUSION JAILBREAK (LFJ) introduces Hidden State Interpolation (HSI), which mathematically fuses harmful and benign representations. This “semantic superposition” masks malicious intent within the latent space, achieving superior stealth and alignment bypass compared to prior continuous approaches.

### 2.3 Defenses Against Jailbreaking

Defenses have evolved from RLHF-based alignment (Ouyang et al., 2022) to inference-time mechanisms like *SmoothLLM* (Robey et al., 2023) and *ASF* (Khachaturov and Mullins, 2025), with the latter filtering malicious suffixes via prompt segmentation. However, these defenses primarily address input-level or discrete patterns. We demonstrate that *latent-space attacks* bypass such paradigms by manipulating internal representations without detectable input artifacts. To counter this, we propose *latent adversarial training* as a targeted defense for this emerging vulnerability.

## 3 Preliminaries

### 3.1 Notation and Problem Formulation

Let  $f_\theta$  denote a safety-aligned LLM parameterized by weights  $\theta$ . Given an input sequence of tokens  $x = \{x_1, \dots, x_n\}$ , the model processes information through  $L$  stacked layers to compute the probability distribution of the next token autoregressively.

Crucially for our method, we focus on the internal representations. We denote the hidden state (or activation) of the  $i$ -th token at the  $l$ -th layer as  $\mathbf{h}_i^{(l)} \in \mathbb{R}^d$ , where  $d$  is the hidden dimension. The forward propagation from layer  $l$  to  $l + 1$  can be abstracted as:

$$\mathbf{h}_i^{(l+1)} = \text{LayerBlock}_l(\mathbf{h}_1^{(l)}, \dots, \mathbf{h}_i^{(l)}), \quad (1)$$

where  $\text{LayerBlock}_l$  encompasses the standard multi-head self-attention and feed-forward mechanisms. The final output is generated based on the hidden states of the last layer.

The objective of a jailbreak attack is to identify a perturbation strategy that maximizes the likelihood of generating a target harmful response  $y$  given a malicious query  $x_{mal}$ , effectively bypassing the safety alignment embedded in  $f_\theta$ . Formally, we aim to maximize  $P(y|\text{Attack}(x_{mal}); \theta)$ .

### 3.2 Threat Model

Following standard protocols in adversarial NLP (Zou et al., 2023b), we operate under a **white-box** setting. We assume the adversary possesses the following capabilities: (1) Read Access: The adversary can access the model’s internal representations (hidden states  $\mathbf{h}$ ) and compute gradients of the loss with respect to these states ( $\nabla_{\mathbf{h}}\mathcal{L}$ ). (2) Inference-Time Intervention: The adversary can modify the hidden states during the forward pass (e.g., via activation steering or, in our case, interpolation).

However, strictly adhering to practical attack constraints, the adversary does not have modify ac-

cess to the model parameters  $\theta$  (i.e., no fine-tuning is allowed) and cannot alter the model architecture.

## 4 Latent Fusion Jailbreak

### 4.1 Overview and Problem Formulation

To elicit a target harmful response  $y$  from a safety-aligned LLM  $f_\theta$ , we propose LATENT FUSION JAILBREAK (LFJ). Unlike discrete optimization methods (Zou et al., 2023b) that are computationally expensive and yield high-perplexity artifacts, LFJ operates directly within the continuous hidden state space to bypass safety alignment efficiently.

The core intuition of LFJ is *Semantic Camouflage*: by mathematically fusing the activation patterns of  $x_{harm}$  with a thematically similar benign query  $x_{benign}$ , we construct a hybrid representation that retains the malicious semantic drive but evades safety filters that detect refusal-inducing features. Formally, we seek to optimize a set of layer-wise fusion coefficients  $\alpha$  such that:

$$\min_{\alpha} \mathcal{L}_{\text{attack}}(f_\theta(\text{Fuse}(x_{\text{harm}}, x_{\text{benign}}; \alpha)), y) + \lambda \mathcal{R}(\alpha) \quad (2)$$

where  $\text{Fuse}(\cdot)$  is our interpolation mechanism and  $\mathcal{R}$  is a regularization term ensuring fluency.

### 4.2 Thematic Query Pairing

To ensure that the interpolated representations reside on a plausible semantic manifold of the language model, we identify pairs of harmful queries ( $q_h$ ) and benign queries ( $q_b$ ) that share congruent syntactic and semantic structures. This design draws upon recent findings in representation engineering, which suggest that steering internal activations along specific semantic directions can effectively bypass safety guardrails (Zou et al., 2023a; Zhou et al., 2024a). Unlike random pairing, which often leads to distributional collapse or detectable anomalies (Zhao et al., 2024), our thematic matching strategy ensures that  $q_b$  mirrors the logical flow of  $q_h$  while pivoting to a safe intent (e.g., transforming “building a bomb” into “building a cake”).

Specifically, following the paradigm of leveraging LLMs for adversarial generation (Chao et al., 2023; Liu et al., 2023), we utilize an auxiliary LLM (e.g., GPT-3.5) to generate  $q_b$  by prompting it to structuralize the benign query based on the template of  $q_h$ . To maintain thematic coherence, we enforce a quantitative constraint using the cosine similarity of mean-pooled token embeddings  $e(q)$  from

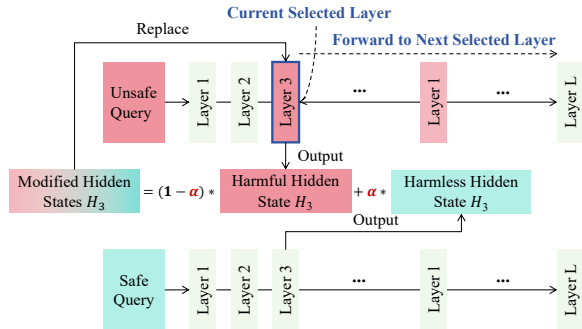


Figure 3: Layer-wise Hidden State Interpolation Process

a pre-trained BERT model (Devlin et al., 2018):

$$\text{sim}(q_h, q_b) = \frac{e(q_h) \cdot e(q_b)}{\|e(q_h)\| \|e(q_b)\|} \geq 0.8, \quad (3)$$

where a threshold of 0.8 is established to filter out pairs with insufficient relevance. This structural and semantic alignment serves to minimize the Euclidean distance between their hidden states  $\|\mathbf{h}_h - \mathbf{h}_b\|_2$ , thereby ensuring that the resulting fused representations yield coherent transitions and robust safety boundaries within the latent space.

### 4.3 Gradient-Guided Hidden State Interpolation

As illustrated in Figure 3, we propose a targeted mechanism to selectively fuse hidden states at critical layers. Let  $\mathbf{h}_i^{(l)} \in \mathbb{R}^d$  denote the representation of the  $i$ -th token at layer  $l$ .

**Sensitivity-Based Layer Selection.** Not all layers contribute equally to the model’s refusal behavior; recent studies indicate that safety alignment is often encoded in specific “safety layers” or neuronal subspaces (Zhou et al., 2024a; Zou et al., 2023a). To identify these critical layers efficiently, we perform a sensitivity analysis using a refusal loss  $\mathcal{L}_{ref}$ . This loss maximizes the probability of generating standard rejection tokens  $W_r = \{\text{“Sorry”, “unable”, “illegal”}\}$ , a set commonly used to demarcate refusal boundaries (Zou et al., 2023b). Given a harmful query  $q_h$ , the importance score  $S(l)$  for each layer is computed as the aggregate gradient norm:

$$S(l) = \sum_i \left\| \frac{\partial \mathcal{L}_{ref}}{\partial \mathbf{h}_i^{(l)}} \right\|_2. \quad (4)$$

Following the statistical thresholding strategy, we select layers where  $S(l) > \bar{S} + \sigma_S$  as the set of intervention layers  $\mathcal{L}_{edit}$ . This targeted approach

disrupts safety mechanisms while minimizing perturbations to the model’s general linguistic capabilities.

**Semantic Fusion and Optimization.** For each  $l \in \mathcal{L}_{edit}$ , we construct the hybrid hidden state  $\tilde{\mathbf{h}}^{(l)}$  via a layer-specific interpolation coefficient  $\alpha^{(l)} \in [0, 1]$ :

$$\tilde{\mathbf{h}}_i^{(l)} = (1 - \alpha^{(l)})\mathbf{h}_{i,harm}^{(l)} + \alpha^{(l)}\mathbf{h}_{i,benign}^{(l)}. \quad (5)$$

This operation effectively projects the harmful representation toward the benign subspace, drawing on principles of activation steering (Zou et al., 2023a). To balance refusal suppression with response quality, we optimize  $\alpha$  by minimizing:

$$\mathcal{L}_{total} = \mathcal{L}_{target}(\tilde{y}, y) - \beta \sum_{w \in W_r} \log P(w|\tilde{\mathbf{h}}) + \gamma \|\alpha\|_2, \quad (6)$$

where  $\beta$  and  $\gamma$  control the rejection penalty and regularization strength, respectively. The explicit penalization of refusal tokens aligns with the optimization strategy employed in *DSN* (Zhou et al., 2024a). Crucially, unlike soft-prompt or latent optimization methods (e.g., *GBDA* or *PEZ*) that operate in unconstrained spaces and risk generating gibberish (Guo et al., 2021; Wen et al., 2024), our interpolation is strictly constrained between two valid natural language manifolds, inherently preserving token-level fluency.

#### 4.4 Token Generation and Iteration

After hidden state interpolation, we generate the output sequence autoregressively. From the interpolated hidden states  $h_i^{(l)}(\hat{q})$ , we compute logits by propagating through the LLM’s remaining layers and output head. The next token  $w_i$  is selected using top- $k$  sampling with  $k = 40$ , ensuring a balance between diversity and coherence.

To enforce adversarial compliance, we employ a rejection-sampling strategy similar to inference-time interventions (Huang et al., 2023). Specifically, if  $w_i$  belongs to the standard rejection set  $W_r = \{\text{“apologize”}, \text{“unable”}, \text{“illegal”}\}$ , we discard it and resample up to  $\text{max\_attempts} = 10$  times. If no valid token is found, we halt and output the current sequence. The sequence updates as:

$$\{w_1, \dots, w_{i-1}\} \rightarrow \{w_1, \dots, w_{i-1}, w_i\}, \quad (7)$$

where  $w_i$  is the selected token. Generation proceeds until an end-of-sequence token  $\langle \text{EOS} \rangle$  or the maximum length  $n$  is reached.

## 5 Adversarial Training Defense

To mitigate LFJ’s vulnerabilities in bypassing safety guardrails via HSI, we propose a targeted adversarial training framework. Inspired by robust optimization principles (Jain et al., 2023), it fine-tunes the LLM on synthetic adversarial examples, forcing perturbed latent representations back to the safety manifold and neutralizing harmful queries while preserving performance on benign inputs.

### 5.1 Latent Adversarial Data Generation

We construct an adversarial dataset  $\mathcal{D}_{adv}$  by simulating the latent space perturbations characteristic of LFJ. Specifically, we identify pairs of harmful queries ( $q_h$ ) and benign “mask” queries ( $q_b$ ) that exhibit high semantic and structural alignment. For instance, a malicious intent (e.g., synthesizing explosives) is paired with a structurally similar safe topic (e.g., formulating cleaning solutions).

To generate the training samples, we perform HSI at critical layers  $\{l_1, \dots, l_k\}$ , which are selected based on high gradient sensitivity scores (as defined in §4). The fused hidden state  $\mathbf{h}_i^{(l_j)}(\hat{q})$  is computed as:

$$\mathbf{h}_i^{(l_j)}(\hat{q}) = (1 - \alpha^{(l_j)})\mathbf{h}_i^{(l_j)}(q_h) + \alpha^{(l_j)}\mathbf{h}_i^{(l_j)}(q_b), \quad (8)$$

where the mixing coefficient  $\alpha^{(l_j)}$  is sampled from a uniform distribution  $\alpha \sim \mathcal{U}[0.2, 0.8]$  to cover a diverse range of fusion intensities.

The resulting dataset  $\mathcal{D}_{adv}$  comprises 1,000 pairs of  $(\hat{q}, y_{safe})$ , where  $\hat{q}$  represents the latent-fused query and  $y_{safe}$  denotes a standard refusal response. To ensure training stability, we enforce strict coherence constraints during pair selection: query pairs must satisfy a BERT-based cosine similarity  $\geq 0.8$  (Devlin et al., 2018) and a dependency tree overlap  $\geq 70\%$ .

### 5.2 Training Objective

The training objective is formulated to reconcile the trade-off between adversarial robustness and general linguistic capability (Madry et al., 2017). We employ a multi-objective loss function that jointly optimizes for performance on benign instructions and resistance to jailbreak attempts. The total loss  $\mathcal{L}_{total}$  is defined as a weighted summation:

$$\mathcal{L}_{total} = 0.7\mathcal{L}_{benign}(\theta, \mathcal{D}_{benign}) + 0.3\mathcal{L}_{adv}(\theta, \mathcal{D}_{adv}), \quad (9)$$

where  $\mathcal{L}_{benign}$  represents the standard cross-entropy loss over the benign dataset  $\mathcal{D}_{benign}$ , ensuring the

model maintains its helpfulness and utility (Ouyang et al., 2022).

The adversarial loss,  $\mathcal{L}_{\text{adv}}$ , is specifically designed to enforce safety alignment. Unlike attacks that suppress refusal features (Zhou et al., 2024a), our objective explicitly encourages the generation of safety-compliant responses ( $y_{\text{safe}}$ ) and increases the likelihood of refusal tokens ( $W_r$ ) when the model is challenged with adversarial inputs  $\hat{q}$ . This aligns with recent directed representation optimization strategies (Zheng et al., 2024). The adversarial loss is calculated as:

$$\mathcal{L}_{\text{adv}} = - \sum_{(\hat{q}, y_{\text{safe}}) \in \mathcal{D}_{\text{adv}}} \log P(y_{\text{safe}} | \hat{q}; \theta) - 0.5 \sum_{w \in W_r} \log P(w | \hat{q}; \theta). \quad (10)$$

By minimizing this objective, the model learns to map perturbed latent states back to the refusal manifold, thereby neutralizing the attack while preserving generation quality on benign user queries. Explanation of Changes and Citations

## 6 Experiment

To address the limitations of discrete optimization attacks, this study investigates three core questions:

- **RQ1** (Effectiveness): Can latent representation manipulation achieve higher attack success rates and linguistic fluency than token-level optimization?
- **RQ2** (Mechanism): How does hidden state interpolation “mask” malicious intent to circumvent refusal mechanisms?
- **RQ3** (Defense): Can latent adversarial training mitigate these vulnerabilities without compromising general model utility?

### 6.1 Experiment Setup

**Dataset.** We evaluate Lfj on four widely-used safety benchmarks targeting LLM vulnerabilities: *AdvBench* (Zou et al., 2023b), *MaliciousInstruct* (Huang et al., 2023), *PKU-Alignment* (Ji et al., 2023), and *ToxicChat* (Lin et al., 2023). *AdvBench* contains 520 adversarial queries across diverse harmful categories. *MaliciousInstruct* includes 100 prompts spanning 10 real-world malicious intents.

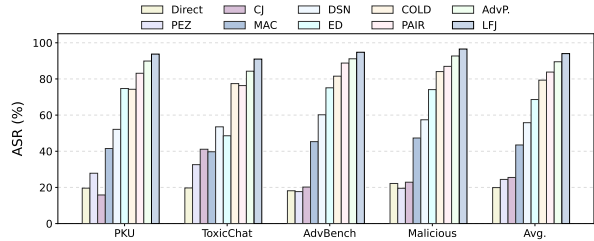


Figure 4: Attack Success Rate (ASR) comparison across different methods on multiple datasets.

**Models.** We evaluate Lfj on five open-source LLMs with diverse architectures and alignment strategies: Vicuna-7B<sup>1</sup> (Chiang et al., 2023), LLaMA-2-7B-Chat<sup>2</sup> (Touvron et al., 2023), Guanaco-7B<sup>3</sup> (Detmeters et al., 2024), LLaMA-3-70B<sup>4</sup> (Dubey et al., 2024), and Mistral-7B-Instruct<sup>5</sup> (Jiang et al., 2023).

**Implementation Details.** For the adversarial training defense, we fine-tune the target LLM using Low-Rank Adaptation (LoRA) on a balanced dataset comprising 1,000 adversarial ( $\mathcal{D}_{\text{adv}}$ ) and 1,000 benign ( $\mathcal{D}_{\text{benign}}$ ) examples. This setup ensures the model learns robust decision boundaries without catastrophic forgetting. Detailed hyperparameters, decoding strategies, and hardware configurations are provided in Appendix.

**Evaluation Metrics and Baselines.** To evaluate alignment degradation, we use Attack Success Rate (ASR), defined as the proportion of adversarial prompts that elicit policy-violating responses, as judged by DEEPSEEK-V3 (et al., 2024). A response is considered policy-violating (successful jailbreak) if it meets specific criteria for harmfulness and quality. We benchmark Lfj against four SOTA attack paradigms: (1) Prompt-Based: Adversarial inputs like *PAIR* (Chao et al., 2023), *AdvPrompter* (Paulus et al., 2025), *MAC* (Zhang and Wei, 2025), and *Emulated Decision* (Zhou et al., 2024b). (2) Representation-Based: State manipulation via internal activations, e.g., *DSN* (Zhou et al., 2024a). (3) Parameter-Based: Parameter/training exploits like *PEZ* (Wen et al., 2024) (PEFT-induced) and *CJ* (Huang et al., 2023) (align-

<sup>1</sup><https://huggingface.co/lmsys/vicuna-7b-v1.5>

<sup>2</sup><https://huggingface.co/meta-llama/llama-2-7b-chat-hf>

<sup>3</sup><https://huggingface.co/timdettmers/guanaco-7b>

<sup>4</sup><https://huggingface.co/meta-llama/Meta-Llama-3-70B-Instruct>

<sup>5</sup><https://huggingface.co/mistralai/Mistral-7B-Instruct-v0.1>

ment degradation). (4) Decoding-Based: Controlled generation dynamics, e.g., energy-based *COLD* (Qin et al., 2022) sampling.

## 6.2 RQ1: Jailbreak Effectiveness

Figure 4 illustrates the comparative ASR of our proposed LFJ against state-of-the-art baselines across five safety-aligned LLMs.

**Superiority over Discrete Optimization..** As shown in Figure 4, LFJ achieves a global average ASR of **94.01%**, significantly outperforming prompt-based optimization methods such as *AdvPrompter* (89.51%) and *PAIR* (83.80%). While discrete attacks like *GCG* often struggle with the combinatorial complexity of token search—resulting in high computational costs and often incoherent gibberish (Zou et al., 2023b)—LFJ leverages the continuous nature of the latent space. By performing gradient-guided interpolation, LFJ avoids the local optima inherent in discrete optimization, allowing for smoother and more effective traversal across the safety decision boundary.

**Comparison with Representation Engineering..** Crucially, LFJ demonstrates a substantial advantage over existing representation-level attacks like *DSN* (Zhou et al., 2024a), which averages only 55.81% ASR. This performance gap highlights a fundamental difference in attack philosophy: *DSN* attempts to *suppress* the model’s refusal direction, which strong safety alignment can often resist. In contrast, LFJ employs *HSI* to blend harmful intents with benign semantic structures. This creates a “camouflage” effect in the latent space, effectively deceiving the model’s safety filters rather than forcefully suppressing them.

**Robustness Against Strong Alignment..** Notably, LFJ exhibits exceptional potency on models known for rigorous safety alignment, such as Mistral-7B and LLaMA-2. On the *Malicious* dataset, LFJ achieves near-perfect success rates on Mistral (97.80%) and Vicuna (98.20%), whereas baselines like *ED* and *DSN* degrade significantly (e.g., *DSN* drops to 50.03% on Mistral). This suggests that while current safety alignment techniques (e.g., RLHF) are effective at filtering surface-level adversarial prompts, they remain vulnerable to deep latent perturbations that mimic benign representations.

## 6.3 RQ2: Mechanism

**Query Pair Selection.** To evaluate LFJ’s query pair selection, we ablate three key components:

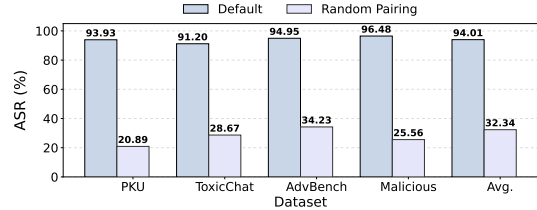


Figure 5: Ablation study on query pair selection in LFJ.

thematic similarity, syntactic similarity, and LLM-generated benign queries, measuring their impact on ASR. As shown in Figure 5, full LFJ achieves 94.01% average ASR, while random pairing with unrelated benign queries drops to 32.34%, underscoring the importance of targeted selection. Results confirm that both thematic and syntactic similarities are critical, with thematic similarity playing a dominant role.

### Ablation Study on Hidden State Interpolation.

To assess HSI components in LFJ, we ablate: (1) gradient-based layer selection, (2) gradient-based token selection, and (3) sequential forward propagation. Experiments use five model families on *PKU*, *ToxicChat*, *AdvBench*, and *Malicious* datasets.

For layer selection ( $S^{(l)} > \bar{S} + \sigma_S$ ), we test: (a) *Uniform Interpolation* ( $\alpha = 0.1$  across all layers); (b) *Random Layers* (random  $k$  layers); (c) *Fixed Layers* (first/last 5 layers). For tokens, apply HSI to all in selected layers, ignoring  $G_i^{(l_j)} > \bar{G}^{(l_j)} + \sigma^{(l_j)}$ . For propagation, perform simultaneous HSI with one forward pass.

Table 1 shows results. *Default* LFJ yields highest ASR (avg. 94.01%). *Uniform Interpolation* drops to 28.07%, due to weak perturbations. *Random Layers* reduces by 61% (to 32.69%), failing safety targeting. *Fixed Shallow/Deep Layers* perform worse (29.94%/37.94%), with deep better but suboptimal. *Without Token Selection*: 40.04% (54% drop), harming precision. *Without Sequential Prop.*: 35.98% (58% drop), disrupting coherence.

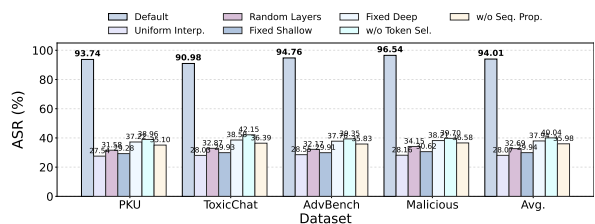


Figure 6: Ablation on HSI in LFJ across datasets. Removing key components significantly lowers Attack Success Rate (ASR). ↓ indicates the drop relative to Default.

Table 1: Ablation on HSI in LFJ across datasets. Removing key components significantly lowers Attack Success Rate (ASR). ↓ indicates the drop relative to Default.

Method	PKU	ToxicChat	AdvBench	Malicious	Avg.
<b>Default</b>	<b>93.74</b>	<b>90.98</b>	<b>94.10</b>	<b>96.54</b>	<b>94.01</b>
Uniform Interp.	27.54	28.03	28.55	28.16	28.07 (↓65.9)
Random Layers	31.58	32.87	32.17	34.15	32.69 (↓61.3)
Fixed Shallow	29.28	29.93	29.91	30.62	29.94 (↓64.1)
Fixed Deep	37.22	38.58	37.76	38.21	37.94 (↓56.1)
w/o Token Sel.	38.96	42.15	39.35	39.70	40.04 (↓54.0)
w/o Seq. Prop.	35.10	36.39	35.83	36.58	35.98 (↓58.0)

Table 2: Ablation on Optimization Components. ASR (%) measures attack success, while Avg. PPL assesses fluency. ↓ denotes performance drop.

Variant	PKU	ToxicChat	AdvBench	Avg. ASR	Avg. PPL
<b>Default</b>	<b>93.74</b>	<b>90.98</b>	<b>94.10</b>	<b>94.01</b>	<b>5.2</b>
w/o Fluency	87.12	85.45	89.90	88.45 (↓5.6)	12.3
w/o Comp.	89.56	88.78	91.12	90.67 (↓3.3)	6.1
Fixed $\alpha$	70.89	68.67	74.23	72.34 (↓21.7)	8.5
w/o Masking	75.34	73.12	78.67	76.78 (↓17.2)	7.2

**Ablation Study on Optimization with Gradient Masking.** To investigate the optimization process in LFJ, we conduct ablations on key loss components and mechanisms, including (1) removing the fluency term by setting  $\lambda_1 = 0$  (i.e., omitting  $\mathcal{L}_{\text{fluency}}$ ), which eliminates the perplexity penalty and assesses the trade-off between ASR and fluency; (2) removing the computational term by setting  $\lambda_2 = 0$  (i.e., omitting  $\mathcal{L}_{\text{comp}}$ ), which removes the penalty on layer usage and tends to increase the number of layers  $k$  and computational cost; (3) fixing the interpolation weight to a constant  $\alpha = 0.5$ , disabling optimization; and (4) disabling gradient masking, allowing gradients to update LLM parameters, which risks compromising model integrity. Table 2 shows results. *Default*: 94.01% avg. ASR, 5.2 PPL. *w/o Fluency*: 88.45% ASR, 12.3 PPL (ASR drop with higher PPL, indicating fluency is key for success). *w/o Comp.*: 90.67% ASR, 6.1 PPL (slight ASR drop, higher compute due to more layers). *Fixed Alphas*: 72.34% ASR, 8.5 PPL (major ASR drop, reduced fluency). *w/o Masking*: 76.78% ASR, 7.2 PPL (ASR drop, compromises stealth and integrity).

#### 6.4 RQ3: Defense

To evaluate the effectiveness of our proposed adversarial training against LFJ attacks, we fine-tune the LLaMA-2-7B model using adversarial examples generated via the HSI method. Model robustness

Table 3: Defense Effectiveness (ASR %) Ablation. Lower ASR indicates better defense. ↓ denotes the reduction in ASR compared to the Baseline.

Variant	PKU	ToxicChat	AdvBench	Malicious	Avg.
<b>Baseline</b>	93.74	90.98	94.10	94.10	94.01
<b>Full Defense</b>	<b>11.12</b>	<b>10.45</b>	<b>13.90</b>	<b>14.33</b>	<b>12.45</b> (↓81.6)
<b>w/o Adv. Loss</b>	84.56	82.78	87.12	88.23	85.67 (↓8.3)
<b>w/o Rejection</b>	27.89	26.67	29.23	30.56	28.34 (↓65.7)

is measured by the reduction in ASR under LFJ attacks, while ensuring minimal degradation on benign inputs. The latter is assessed through perplexity on standard benchmarks (e.g., *GLUE*) and the refusal rate on benign queries.

We compare the full defense setup with several ablation variants. As shown in Table 3, the baseline model exhibits high vulnerability, with an average ASR of 94.01%. In contrast, our full defense setup significantly reduces the ASR to 12.45%, demonstrating effective mitigation while maintaining benign behavior (e.g., refusal rate on benign queries remains below 5%). Removing the adversarial loss leads to a high ASR of 85.67%, highlighting the importance of incorporating adversarial examples during training. Excluding the rejection encouragement term results in an ASR of 28.34%, indicating that explicitly promoting refusal behavior further enhances robustness.

## 7 Conclusion

In this paper, we have introduced LATENT FUSION JAILBREAK (LFJ), a method for bypassing safety alignments in LLMs through the interpolation of hidden states from harmful and benign query pairs. By incorporating thematic and syntactic similarities in query selection, gradient-guided hidden state manipulation, and optimized parameters balancing attack success with fluency and efficiency, LFJ demonstrates superior performance, achieving an average attack success rate of 94.01% across multiple benchmarks and models. This outperforms existing jailbreak techniques, highlighting the vulnerabilities in current safety mechanisms that operate primarily at the input level. To address these risks, we proposed an adversarial training approach that fine-tunes models on interpolated examples, effectively reducing the attack success rate by more than 80% while maintaining functionality on standard inputs.

## Limitations

While LATENT FUSION JAILBREAK demonstrates high efficacy in uncovering vulnerabilities within aligned LLMs, we acknowledge several limitations in our current methodology:

**White-Box Dependency.** The core mechanism of LFJ relies on gradient-guided identification of safety-critical layers and tokens to perform Hidden State Interpolation (Zou et al., 2023b). Specifically, the calculation of gradient norm scores (Eq. 6) necessitates access to the model’s internal weights and backpropagation gradients. This restricts the direct application of LFJ optimization to open-source models.

**Computational Overhead.** Compared to static prompt injection or manual template-based attacks (e.g., DAN), LFJ incurs higher computational costs during the attack generation phase. The iterative optimization of the interpolation coefficient  $\alpha$  and the forward/backward passes required for layer selection increase inference latency. Although LFJ is more efficient than discrete token optimization methods like GCG (Zou et al., 2023b) due to the continuous nature of the latent space, it still requires GPU resources that may not be available for all adversarial testing scenarios.

**Defense Trade-offs.** Our proposed adversarial training defense significantly reduces the ASR against LFJ. However, as observed in prior adversarial training studies (Jain et al., 2023), robust optimization can sometimes incur an "alignment tax," potentially leading to a slight degradation in the model’s capability on complex benign instructions or increasing the rate of false refusals (over-defensiveness). Future work is needed to explore more disentangled representation editing methods to minimize this trade-off.

**Scope of Modality.** Currently, LFJ is tailored specifically for textual LLMs. With the rise of Multimodal Large Language Models (MLLMs), it remains to be explored whether fusing latent representations across different modalities (e.g., vision and text) would yield similar or more potent jailbreaking effects. Extending HSI to multimodal alignment remains a direction for future research.

## Potential Risks

**lowering the Bar for Malicious Use.** The primary risk associated with LFJ is that it significantly lowers the technical barrier for malicious actors to bypass LLM safety guardrails. As demonstrated in

our experiments, LFJ achieves a 94.01% average ASR on benchmarks covering sensitive topics such as illegal activities, hate speech, and malware generation (Zou et al., 2023b; Huang et al., 2023). Unlike manual jailbreaks (e.g., DAN) that require human ingenuity, or optimization-based attacks (e.g., GCG) that generate easily detectable gibberish, LFJ produces fluent and stealthy prompts automatically. This capability could potentially be exploited to scale up the generation of harmful content or disinformation campaigns.

## References

- Josh Achiam, Steven Adler, Sandhini Agarwal, Lama Ahmad, Ilge Akkaya, Florencia Leoni Aleman, Diogo Almeida, Janko Altschmidt, Sam Altman, Shyamal Anadkat, et al. 2023. Gpt-4 technical report. *arXiv preprint arXiv:2303.08774*.
- Gabriel Alon and Michael Kamfonas. 2023. [Detecting language model attacks with perplexity](#). *Preprint*, arXiv:2308.14132.
- Yuntao Bai, Saurav Kadavath, Sandipan Kundu, Amanda Askell, Jackson Kernion, Andy Jones, Anna Chen, Anna Goldie, Azalia Mirhoseini, Cameron McKinnon, et al. 2022. Constitutional ai: Harmlessness from ai feedback. *arXiv preprint arXiv:2212.08073*.
- Patrick Chao, Alexander Robey, Edgar Dobriban, Hamed Hassani, George J Pappas, and Eric Wong. 2023. Jailbreaking black box large language models in twenty queries. *arXiv preprint arXiv:2310.08419*.
- W.-L. Chiang, Z. Li, Z. Lin, Y. Sheng, Z. Wu, H. Zhang, L. Zheng, S. Zhuang, Y. Zhuang, J. E. Gonzalez, et al. 2023. [Vicuna: An open-source chatbot impressing gpt-4 with 90% chatgpt quality](#). Accessed 14 April 2023.
- Gelei Deng, Yi Liu, Yuekang Li, Kailong Wang, Ying Zhang, Zefeng Li, Haoyu Wang, Tianwei Zhang, and Yang Liu. 2024. Masterkey: Automated jailbreaking of large language model chatbots. In *Proc. ISOC NDSS*.
- Tim Dettmers, Artidoro Pagnoni, Ari Holtzman, and Luke Zettlemoyer. 2024. Qlora: Efficient finetuning of quantized llms. *Advances in Neural Information Processing Systems*, 36.
- Jacob Devlin, Ming-Wei Chang, Kenton Lee, and K Toutanova Bert. 2018. Pre-training of deep bidirectional transformers for language understanding (2018). *arXiv preprint arXiv:1810.04805*.
- Abhimanyu Dubey, Abhinav Jauhri, Abhinav Pandey, Abhishek Kadian, Ahmad Al-Dahle, Aiesha Letman, Akhil Mathur, Alan Schelten, Amy Yang, Angela Fan, et al. 2024. The llama 3 herd of models. *arXiv e-prints*, pages arXiv-2407.

- DeepSeek-AI et al. 2024. [Deepseek-v3 technical report](#). *Preprint*, arXiv:2412.19437.
- Simon Geisler, Tom Wollschläger, Mohamed Hesham Ibrahim Abdalla, Johannes Gasteiger, and Stephan Günnemann. 2024. Attacking large language models with projected gradient descent. *arXiv preprint arXiv:2402.09154*.
- Chuan Guo, Alexandre Sablayrolles, Hervé Jégou, and Douwe Kiela. 2021. Gradient-based adversarial attacks against text transformers. *arXiv preprint arXiv:2104.13733*.
- Kai Hu, Weichen Yu, Yining Li, Tianjun Yao, Xiang Li, Wenhe Liu, Lijun Yu, Zhiqiang Shen, Kai Chen, and Matt Fredrikson. 2024. Efficient llm jailbreak via adaptive dense-to-sparse constrained optimization. *Advances in Neural Information Processing Systems*, 37:23224–23245.
- Yangsibo Huang, Samyak Gupta, Mengzhou Xia, Kai Li, and Danqi Chen. 2023. Catastrophic jailbreak of open-source llms via exploiting generation. *arXiv preprint arXiv:2310.06987*.
- Neel Jain, Avi Schwarzschild, Yuxin Wen, Gowthami Somepalli, John Kirchenbauer, Ping-yeh Chiang, Micah Goldblum, Aniruddha Saha, Jonas Geiping, and Tom Goldstein. 2023. Baseline defenses for adversarial attacks against aligned language models. *arXiv preprint arXiv:2309.00614*.
- Jiaming Ji, Mickel Liu, Juntao Dai, Xuehai Pan, Chi Zhang, Ce Bian, Chi Zhang, Ruiyang Sun, Yizhou Wang, and Yaodong Yang. 2023. Beavertails: Towards improved safety alignment of llm via a human-preference dataset. *arXiv preprint arXiv:2307.04657*.
- Albert Q Jiang, Alexandre Sablayrolles, Arthur Mensch, Chris Bamford, Devendra Singh Chaplot, Diego de las Casas, Florian Bressand, Gianna Lengyel, Guillaume Lample, Lucile Saulnier, et al. 2023. Mistral 7b. *arXiv preprint arXiv:2310.06825*.
- David Khachaturov and Robert Mullins. 2025. Adversarial suffix filtering: a defense pipeline for llms. *arXiv preprint arXiv:2505.09602*.
- Minghao Li, Wenpeng Xing, Yong Liu, Wei Zhang, and Meng Han. 2025a. Optimizing and attacking embodied intelligence: Instruction decomposition and adversarial robustness. In *2025 IEEE International Conference on Multimedia and Expo (ICME)*, pages 1–6. IEEE.
- Ran Li, Hao Wang, and Chengzhi Mao. 2025b. Largo: Latent adversarial reflection through gradient optimization for jailbreaking llms. *arXiv preprint arXiv:2505.10838*.
- Tianlong Li, Xiaoqing Zheng, and Xuanjing Huang. 2024. Open the pandora’s box of llms: Jailbreaking llms through representation engineering. *arXiv preprint arXiv:2401.06824*.
- Zi Lin, Zihan Wang, Yongqi Tong, Yangkun Wang, Yuxin Guo, Yujia Wang, and Jingbo Shang. 2023. Toxicchat: Unveiling hidden challenges of toxicity detection in real-world user-ai conversation. *arXiv preprint arXiv:2310.17389*.
- Xiaogeng Liu, Nan Xu, Muhao Chen, and Chaowei Xiao. 2023. Autodan: Generating stealthy jailbreak prompts on aligned large language models. *arXiv preprint arXiv:2310.04451*.
- Aleksander Madry, Aleksandar Makelov, Ludwig Schmidt, Dimitris Tsipras, and Adrian Vladu. 2017. Towards deep learning models resistant to adversarial attacks. *arXiv preprint arXiv:1706.06083*.
- Anay Mehrotra, Manolis Zampetakis, Paul Kassianik, Blaine Nelson, Hyrum Anderson, Yaron Singer, and Amin Karbasi. 2024. Tree of attacks: Jailbreaking black-box llms automatically. *Advances in Neural Information Processing Systems*, 37:61065–61105.
- Long Ouyang, Jeffrey Wu, Xu Jiang, Diogo Almeida, Carroll Wainwright, Pamela Mishkin, Chong Zhang, Sandhini Agarwal, Katarina Slama, Alex Ray, et al. 2022. Training language models to follow instructions with human feedback. *Advances in neural information processing systems*, 35:27730–27744.
- Anselm Paulus, Arman Zharmagambetov, Chuan Guo, Brandon Amos, and Yuandong Tian. 2025. [Advprompter: Fast adaptive adversarial prompting for llms](#). *Preprint*, arXiv:2404.16873.
- Lianhui Qin, Sean Welleck, Daniel Khashabi, and Yejin Choi. 2022. Cold decoding: Energy-based constrained text generation with langevin dynamics. *Advances in Neural Information Processing Systems*, 35:9538–9551.
- Alexander Robey, Eric Wong, Hamed Hassani, and George J Pappas. 2023. Smoothllm: Defending large language models against jailbreaking attacks. *arXiv preprint arXiv:2310.03684*.
- Vinu Sankar Sadasivan, Shoumik Saha, Gaurang Sriraman, Priyatham Kattakinda, Atoosa Chegini, and Soheil Feizi. 2024. Fast adversarial attacks on language models in one gpu minute. *arXiv preprint arXiv:2402.15570*.
- Xinyue Shen, Zeyuan Chen, Michael Backes, Yun Shen, and Yang Zhang. 2024. "do anything now": Characterizing and evaluating in-the-wild jailbreak prompts on large language models. In *Proceedings of the 2024 on ACM SIGSAC Conference on Computer and Communications Security*, pages 1671–1685.
- Hugo Touvron, Louis Martin, Kevin Stone, Peter Albert, Amjad Almahairi, Yasmine Babaei, Nikolay Bashlykov, Soumya Batra, Prajjwal Bhargava, Shrutu Bhosale, et al. 2023. Llama 2: Open foundation and fine-tuned chat models. *arXiv preprint arXiv:2307.09288*.

- Alexander Matt Turner, Lisa Thiergart, Gavin Leech, David Udell, Juan J Vazquez, Ulisse Mini, and Monte MacDiarmid. 2023. Steering language models with activation engineering. *arXiv preprint arXiv:2308.10248*.
- Alexander Wei, Nika Haghtalab, and Jacob Steinhardt. 2023. Jailbroken: How does llm safety training fail? *Advances in Neural Information Processing Systems*, 36:80079–80110.
- Yuxin Wen, Neel Jain, John Kirchenbauer, Micah Goldblum, Jonas Geiping, and Tom Goldstein. 2024. Hard prompts made easy: Gradient-based discrete optimization for prompt tuning and discovery. *Advances in Neural Information Processing Systems*, 36.
- Wenpeng Xing, Zhonghao Qi, Yupeng Qin, Yilin Li, Caini Chang, Jiahui Yu, Changting Lin, Zhenzhen Xie, and Meng Han. 2025. Mcp-guard: A defense framework for model context protocol integrity in large language model applications. *arXiv preprint arXiv:2508.10991*.
- Zhenhua Xu, Meng Han, and Wenpeng Xing. 2025a. Evertracer: Hunting stolen large language models via stealthy and robust probabilistic fingerprint. In *Proceedings of the 2025 Conference on Empirical Methods in Natural Language Processing*, pages 7019–7042.
- Zhenhua Xu, Meng Han, Xubin Yue, and Wenpeng Xing. 1906. Insty: a robust multi-level crossgranularity fingerprint embedding algorithm for multi-turn dialogue in large language models. *SCIENTIA SINICA Informationis*, 55(8).
- Zhenhua Xu, Zhebo Wang, Maike Li, Wenpeng Xing, Chunqiang Hu, Chen Zhi, and Meng Han. 2025b. Rap-sm: Robust adversarial prompt via shadow models for copyright verification of large language models. *arXiv preprint arXiv:2505.06304*.
- Zhenhua Xu, Xubin Yue, Zhebo Wang, Qichen Liu, Xixiang Zhao, Jingxuan Zhang, Wenjun Zeng, Wenpeng Xing, Dezhang Kong, Changting Lin, et al. 2025c. Copyright protection for large language models: A survey of methods, challenges, and trends. *arXiv preprint arXiv:2508.11548*.
- Xubin Yue, Zhenhua Xu, Wenpeng Xing, Jiahui Yu, Mohan Li, and Meng Han. 2025. Pree: Towards harmless and adaptive fingerprint editing in large language models via knowledge prefix enhancement. *Preprint*.
- Jingxuan Zhang, Zhenhua Xu, Rui Hu, Wenpeng Xing, Xuhong Zhang, and Meng Han. 2025. Meraser: An effective fingerprint erasure approach for large language models. *arXiv preprint arXiv:2506.12551*.
- Yihao Zhang and Zeming Wei. 2025. Boosting jailbreak attack with momentum. In *ICASSP*.
- Xuandong Zhao, Xianjun Yang, Tianyu Pang, Chao Du, Lei Li, Yu-Xiang Wang, and William Yang Wang. 2024. Weak-to-strong jailbreaking on large language models. *arXiv preprint arXiv:2401.17256*.
- Chujie Zheng, Fan Yin, Hao Zhou, Fandong Meng, Jie Zhou, Kai-Wei Chang, Minlie Huang, and Nanyun Peng. 2024. On prompt-driven safeguarding for large language models. *arXiv preprint arXiv:2401.18018*.
- Yukai Zhou, Zhijie Huang, Feiyang Lu, Zhan Qin, and Wenjie Wang. 2024a. Don’t say no: Jailbreaking llm by suppressing refusal. *arXiv preprint arXiv:2404.16369*.
- Zhanhui Zhou, Jie Liu, Zhichen Dong, Jiaheng Liu, Chao Yang, Wanli Ouyang, and Yu Qiao. 2024b. Emulated disalignment: Safety alignment for large language models may backfire! *arXiv preprint arXiv:2402.12343*.
- Sicheng Zhu, Ruiyi Zhang, Bang An, Gang Wu, Joe Barrow, Zichao Wang, Furong Huang, Ani Nenkova, and Tong Sun. 2023. Autodan: Automatic and interpretable adversarial attacks on large language models. *arXiv preprint arXiv:2310.15140*.
- Andy Zou, Long Phan, Sarah Chen, James Campbell, Phillip Guo, Richard Ren, Alexander Pan, Xuwang Yin, Mantas Mazeika, Ann-Kathrin Dombrowski, et al. 2023a. Representation engineering: A top-down approach to ai transparency. *arXiv preprint arXiv:2310.01405*.
- Andy Zou, Zifan Wang, Nicholas Carlini, Milad Nasr, J Zico Kolter, and Matt Fredrikson. 2023b. Universal and transferable adversarial attacks on aligned language models. *arXiv preprint arXiv:2307.15043*.

## A Attack Configuration

During the generation phase, we employ specific decoding strategies to steer the model. The generation process is guided by rejection lists containing approximately 25–50 terms and affirmative lists of 30–50 terms. If a rejection term is detected with high ranking, the hidden states are modified, and logits are recomputed. We utilize top- $k$  sampling ( $k = 5$ ) with a temperature  $T = 0.7$ . To minimize computational overhead, interpolation is applied exclusively to the final token’s hidden state. All computations are performed in FP16, with a maximum token limit of 500.

## B Defense Training Configuration

For the adversarial training defense, we apply LoRA to safety-critical attention modules (Query, Key, Value) in the higher layers of the LLM. The LoRA configuration uses a rank  $r = 16$  and a scaling factor  $\alpha_{\text{LoRA}} = 32$ . The optimization is

performed using AdamW with a learning rate of  $10^{-5}$  and weight decay of 0.01. We employ a linear learning rate scheduler with a 500-step warmup and gradient clipping with a max norm of 1.0. The training is conducted with a batch size of 16 to maintain the strict 1 : 1 ratio between benign and adversarial examples. The process runs for three epochs with early stopping enabled, updating only the LoRA-adapted weights. All experiments were conducted on a single Nvidia A100 GPU.